

# Regularization and ill-posed problems

Moritz Wolter

July 18, 2016

## 1 Abstract

This report deals with methods to handle perturbations to the right hand side of  $\mathbf{Ax} = \mathbf{b}$ . Precisely an additional noise contribution is added to  $\mathbf{b}$  such that  $\mathbf{b} = \mathbf{b}_{\text{exact}} + \alpha \cdot \mathbf{b}_{\text{noise}}$ . Where  $\mathbf{b}_{\text{noise}}$  is a vector with entries drawn from the standard normal distribution  $\mathcal{N}(0, 1)$  so effectively noise with the distribution  $\mathcal{N}(0, \alpha^2)$  is added. The process of recovering  $\mathbf{x}_{\text{reg}} \approx \mathbf{A}^{-1}\mathbf{b}_{\text{exact}}$  as precisely as possible is called regularization. Tikhonov regularization, TSVD and conjugate gradient methods will be applied and their regularization properties compared. The first two methods require a regularization parameter  $\lambda$ . It can be obtained using for example the L-curve criterion or generalized cross-validation (GCV). Both methods will be explored further.

## 2 Results

### 2.1 Tikhonov regularization

Tikhonov regularization can be implemented using the singular value decomposition of  $\mathbf{A}$ . The idea is to filter out the very small singular values, which are greatly influenced by the noise contribution using

$$\mathbf{x}_{\text{reg}} = \sum_{i=1}^n f_i \frac{\mathbf{u}_i^T \mathbf{b}}{\sigma_i} \mathbf{v}_i. \quad (1)$$

The filter factors  $f_i$  are computed using

$$f_i = \sigma_i^2 / (\sigma_i^2 + \lambda). \quad (2)$$

Where filtering takes place if  $\sigma_i < \lambda$ . On the other hand a singular value  $\sigma$  remains unfiltered if  $\sigma_i > \lambda$ . The equations above can be implemented without a `for` loop in matlab:

```
[U,S,V] = svd(A)
sigma = diag(S);
fVec = sigma.^2 ./ (sigma.^2 + ones(n,1)*lambda.^2);
F = diag(fVec);
x = sum(U*F*diag(sigma.^(-1))*V'*b,2);
```

For this method to work it is essential to choose a good value for  $\lambda$ .

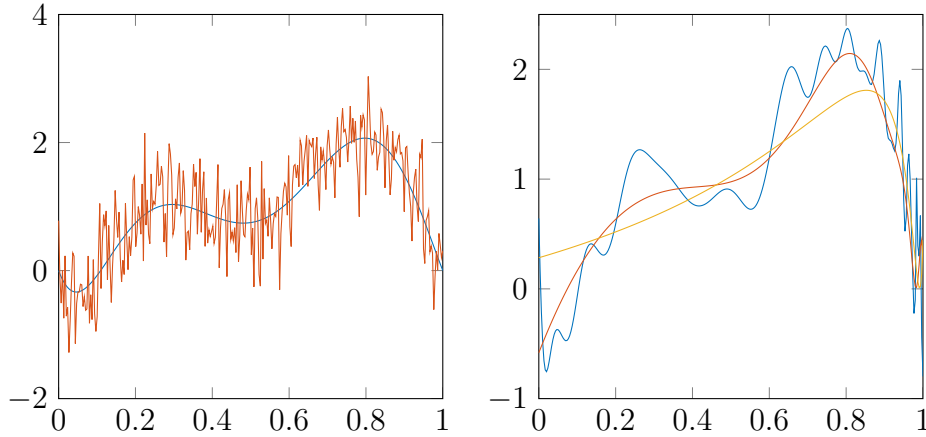


Figure 1: The L-curve in relation to curve fitting problems. On the left a known curve  $\mathbf{b}_{true}$  is shown in blue.  $\mathbf{b} = \mathbf{b}_{true} + \mathbf{b}_{noise}$  is shown in red. The right plot shows efforts to recover the noise free solution. The effects of no filtering (blue,  $\|\mathbf{Ax}\| = 21.77$ ,  $\|\mathbf{Ax} - \mathbf{b}_{true}\| = 7.59$ ), optimal filtering (red,  $\|\mathbf{Ax}\| = 19.44$ ,  $\|\mathbf{Ax} - \mathbf{b}_{true}\| = 3.33$ ) and over-damping (yellow,  $\|\mathbf{Ax}\| = 18.3362$ ,  $\|\mathbf{Ax} - \mathbf{b}_{true}\| = 5.08$ ) are shown.

### 2.1.1 The L-curve

The L-curve is a plot of the residual norm  $\|\mathbf{Ax} - \mathbf{b}\|$  and the norm of the regularized solution  $\|\mathbf{Lx}\|$ . It displays the trade off between the fit to regularized data and the size of the solution and gives insight into the properties of the underlying regularization method.<sup>1</sup> Using Tikhonov regularization as described in equation 1 and the filter of equation 2. The plots in figure 2 have been computed. We are interested in obtaining a result as close to the noise free data as possible. The trade off shown in the L-curve is illustrated in another way in figure 1.<sup>2</sup> When choosing a good filter parameter it is important to remove noise contributions, which is done by minimizing  $\|\mathbf{Lx}\|$ , while at the same time making sure that the data points are still being followed in a satisfactory way, which is done by keeping  $\|\mathbf{Ax} - \mathbf{b}\|$  as small as possible. In practice  $\mathbf{b}_{true}$  is unknown, it has been used in the experiment shown in figure 1 only to verify that the L-curve criterion which has been computed using the noisy  $\mathbf{b}$  is indeed working. The optimal point can be found at the pointy edge of the L-curve, ideally the curvature will display a maximal value here. Following Hansen once more the curvature  $\kappa$  has been computed using<sup>3</sup>

$$\kappa = 2 \cdot \frac{\hat{\rho}'\hat{\eta}'' - \hat{\rho}''\hat{\eta}'}{((\hat{\rho}')^2 + (\hat{\eta}')^2)^{3/2}}. \quad (3)$$

with  $\hat{\eta} = \log(\|x_\lambda\|_2^2)$  and  $\hat{\rho} = \log(\|Ax_\lambda - b\|_2^2)$ . The derivatives have been implemented by simply using right forward differences

$$\hat{\rho}' = \frac{(\hat{\rho}_{k+1} - \hat{\rho}_k)}{(\lambda_{k+1} - \lambda_k)}. \quad (4)$$

<sup>1</sup>The L-curve and its use in the numerical treatment of inverse problems, P. C. Hansen, Department of Mathematical Modelling, Technical University of Denmark, DK-2800 Lyngby, Denmark

<sup>2</sup>following a similar example in: The L-curve and its use in the numerical treatment of inverse problems, P. C. Hansen

<sup>3</sup>The L-curve and its use in the numerical treatment of inverse problems, P. C. Hansen

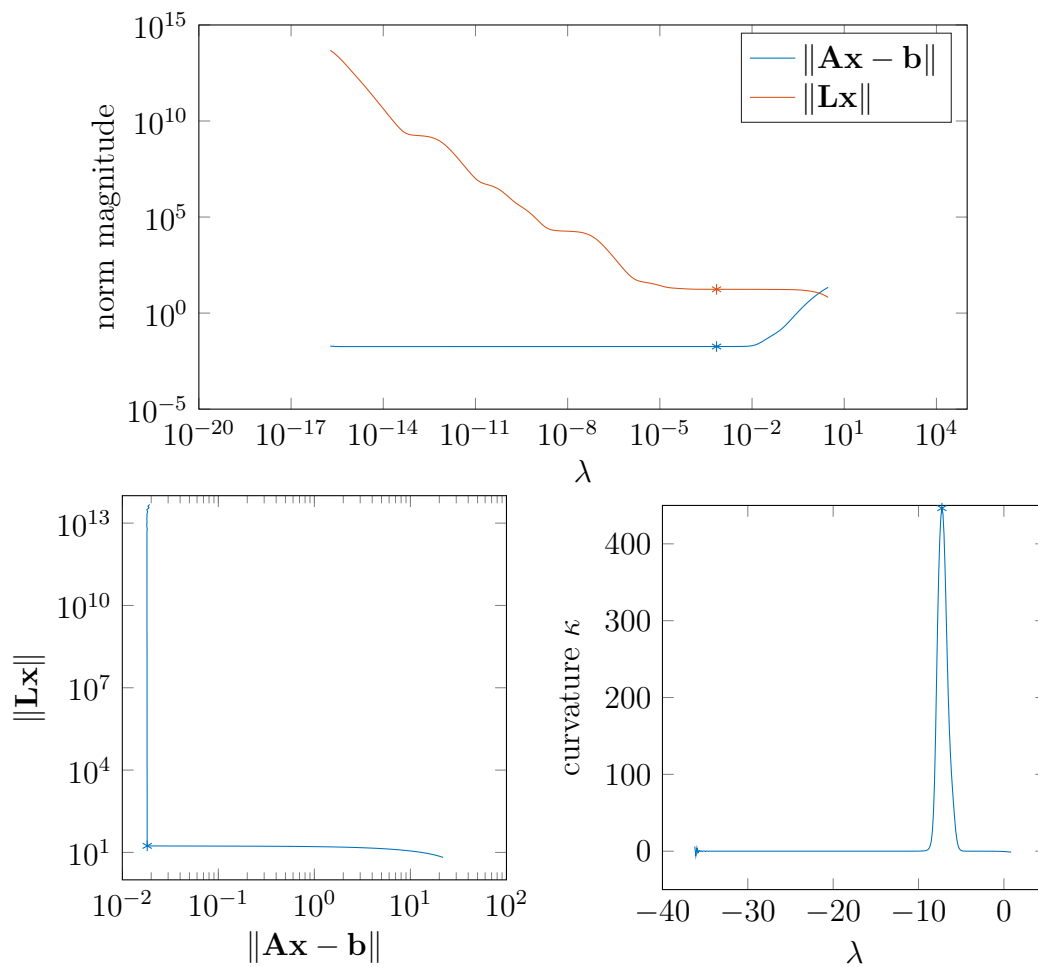


Figure 2: Plots of  $\|\mathbf{Ax} - \mathbf{b}\|$ ,  $\|\mathbf{Lx}\|$  and the curvature of the L-curve  $\kappa$ . For the given **A1**, **berr1** pair.

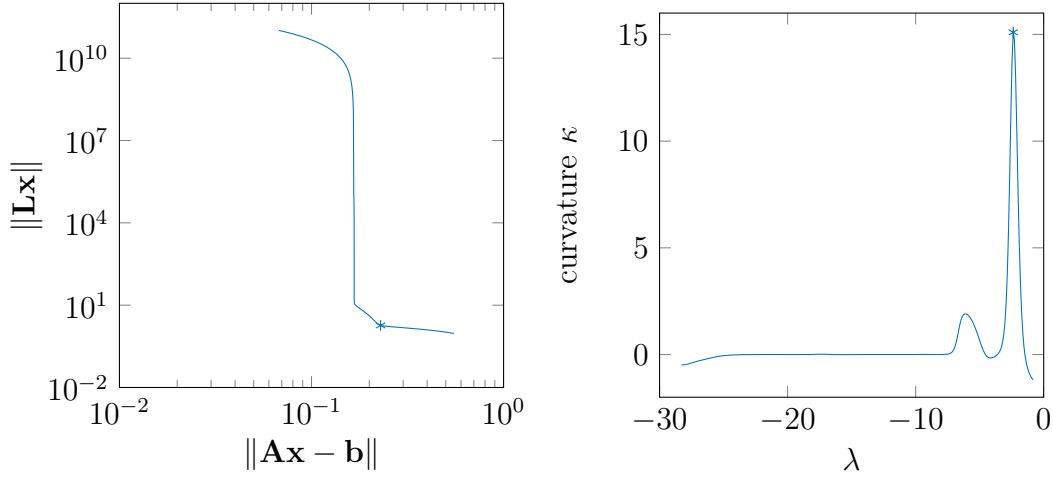


Figure 3: Tikhonov regularization L-curve and curvature for the matrix  $\mathbf{A}_2$  and vector  $\mathbf{b}_{err2}$ .

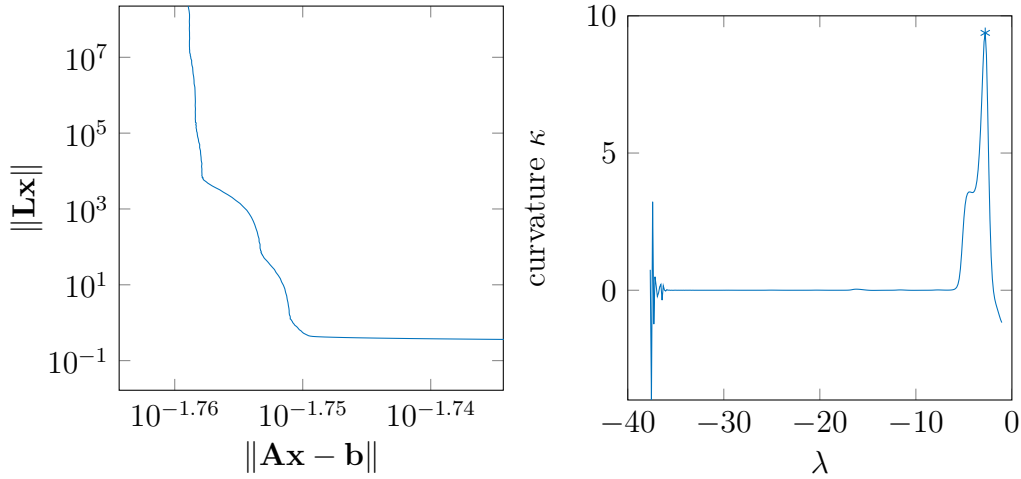


Figure 4: Tikhonov regularization, L-curve and curvature for the matrix  $\mathbf{A}_3$  and vector  $\mathbf{b}_{err3}$ .

For the second derivatives the same process has simply been applied again.  $\hat{\eta}'$  and  $\hat{\eta}''$  have been computed in the same manner. The plot of the curvature which has been obtained by using the formulas above is shown in figure 2 in the bottom left. In all plots in the figure the location of the maximum of  $\kappa$  has been indicated with stars(\*). It is important to notice that  $\lambda$  increases when following the L-curve from the top left to the bottom right.

Figure 3 shows a more dubious case. For the given matrix  $\mathbf{A}_2$  the L-curve displays two edges. The selection criterion now chooses the edge at the bottom as it is curvier then the previous one. However maybe the emphasis should have been to reduce the residual instead of the solution norm. In that case the previous edge should have been selected. This example shows that selection by curvature is not free of flaws, it tends to oversmooth the solution in this case. Figures 5, 6 and 7 show more examples where the L-curve criterion performs very well. However there is an absentee. Matrix  $\mathbf{A}_3$  is missing. Here the L-curve's edged is not found exactly by the curvature based selection criterion,

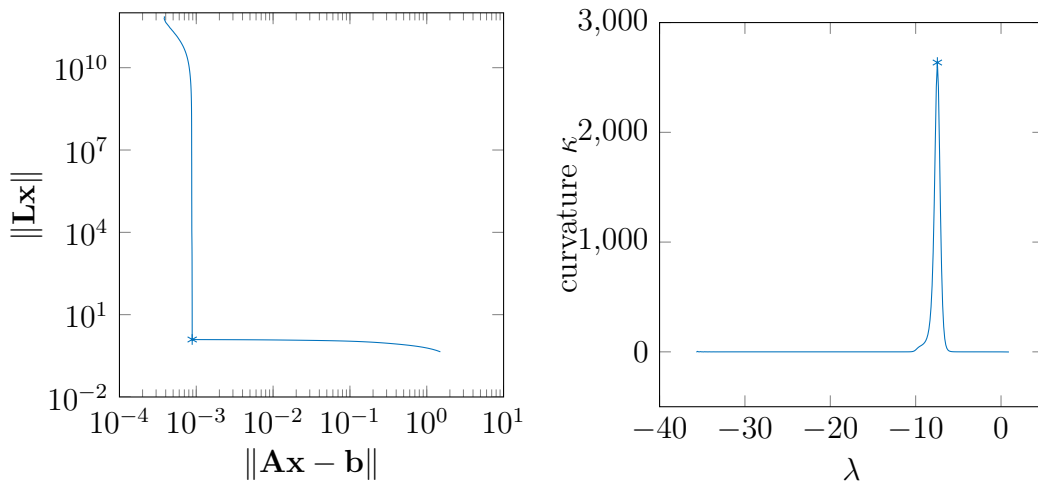


Figure 5: Tikhonov regularization, L-curve and curvature for the matrix  $\mathbf{A}_4$  and vector  $\mathbf{b}_{err4}$ .

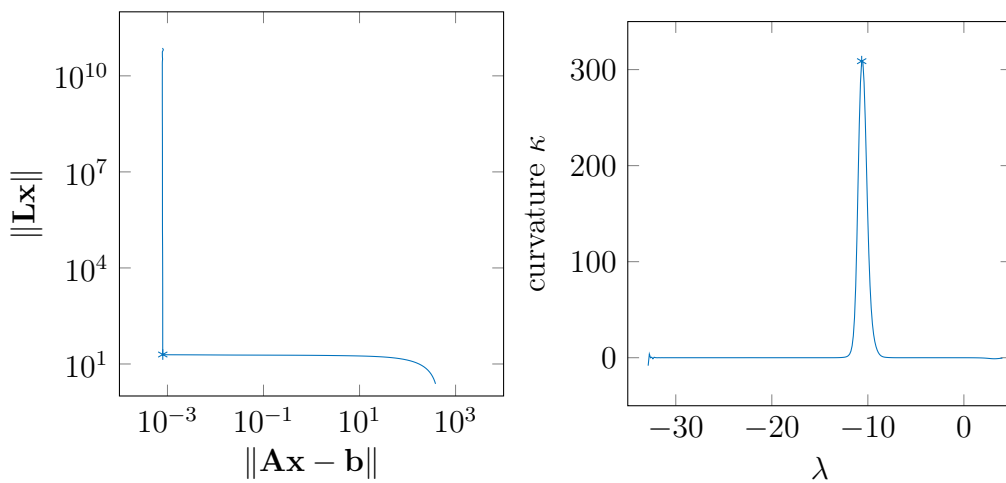


Figure 6: Tikhonov regularization, L-curve and curvature for the matrix  $\mathbf{A}_5$  and vector  $\mathbf{b}_{err5}$ .

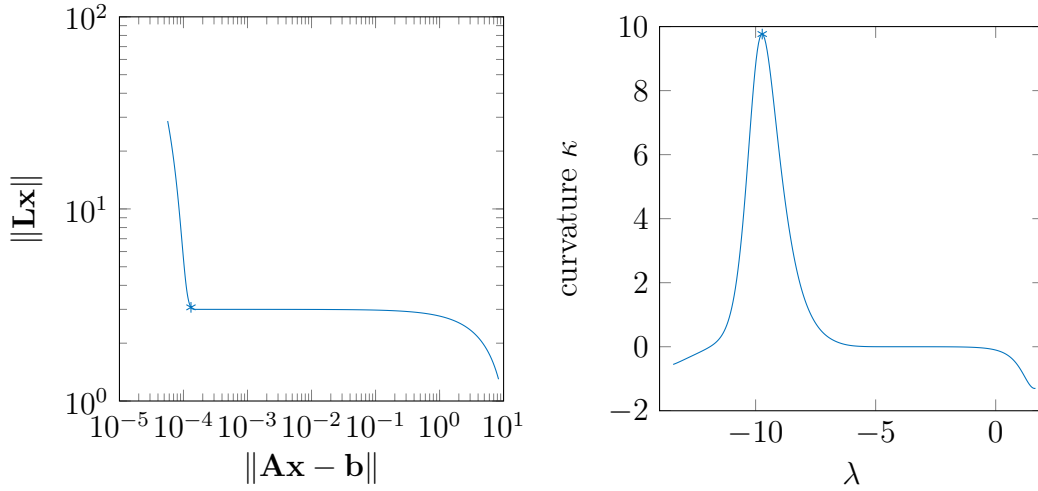


Figure 7: Tikhonov regularization, L-curve and curvature for the matrix  $\mathbf{A}_6$  and vector  $\mathbf{b}_{err6}$ .

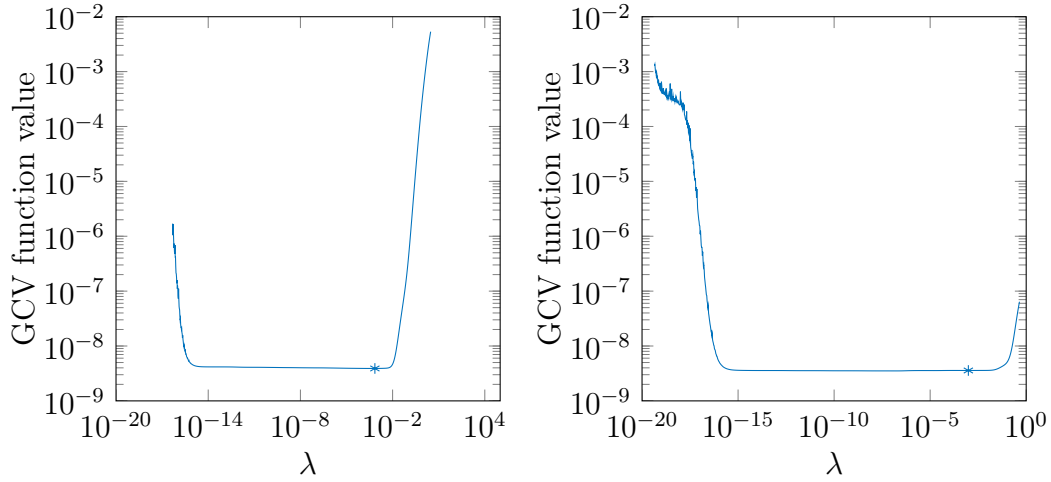


Figure 8: Plot of the value of the GCV-function for different values of  $\lambda$  for the  $\mathbf{A}_1, \mathbf{b}_{err1}$  and the  $\mathbf{A}_3, \mathbf{b}_{err3}$  pair.

this example will be solved using GCV, which as explained in the next section.

## 2.2 Generalized Cross validation (GCV)

An other way to find a suitable regularization parameter is generalized cross validation. When this method is used the function

$$G = \frac{\|\mathbf{Ax}_{reg} - \mathbf{b}\|_2^2}{(\text{trace}(\mathbf{I}_m - \mathbf{AA}^T))^2} \quad (5)$$

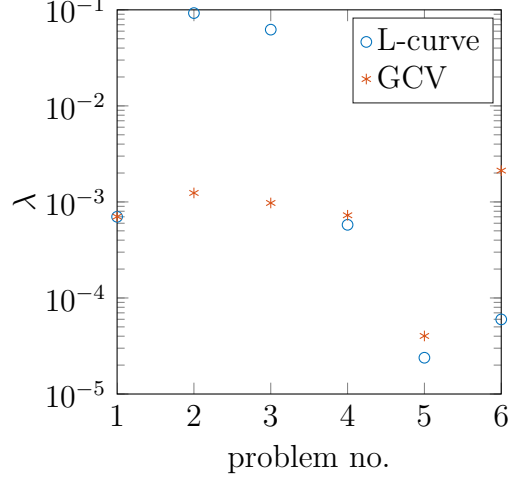


Figure 9: Plot of the lambdas selected by the L-curve curvature criterion and generalized cross validation.

is minimized. With  $\mathbf{x}_{reg}$  defined as in equation 1. The trace of the denominator can be simplified to:

$$\text{trace}(\mathbf{I}_m) - \text{trace}(\mathbf{A}\mathbf{A}^T) \quad \text{assuming symmetry} \quad (6)$$

$$= n - \text{trace}(\mathbf{A}^T \mathbf{A}) \quad (7)$$

$$= n - \text{trace}(\mathbf{V}\mathbf{\Sigma}^T \mathbf{U}^T \mathbf{U} \mathbf{F} \mathbf{\Sigma}^{-1} \mathbf{V}^T) \quad \text{svd} \quad (8)$$

$$= n - \text{trace}(\mathbf{V}^T \mathbf{V} \mathbf{\Sigma}^T \mathbf{F} \mathbf{\Sigma}^{-1}) \quad \text{cyclic rotation} \quad (9)$$

$$= n - \text{trace}(\mathbf{\Sigma}^{-1} \mathbf{\Sigma} \mathbf{F}) \quad \text{cyclic rotation} \quad (10)$$

$$= n - \text{trace}(\mathbf{F}) \quad \mathbf{F} \text{ is diagonal} \quad (11)$$

$$= n - \text{sum}(\mathbf{F}) \quad (12)$$

With  $\mathbf{F}$  being a matrix with the filter factors on the diagonal. The reasoning described above is used to compute the GCV function efficiently. A comparison of the  $\lambda$  values selected by the L-curve curvature criterion and GCV is given in figure 9. For the first problem both methods select almost the same value. In two an three the value selected by the L-curve curvature criterion is significantly larger then what is chosen by the GCV criterion and what a human would have selected. In these six examples this generally happens when the value of the maximum of the  $\kappa$  curve is not very large. In these cases GCV should be preferred.

### 2.3 Picard condition

The Picard condition states that the Fourier coefficients  $|\mathbf{u}_i^T \mathbf{b}|$  have to decay faster then the singular values. If this condition is satisfied, then one has every reason to believe that  $\mathbf{x}_{reg}$  approximates the true  $\mathbf{x}$  well. Figures 10,11,12 show that regularization is necessary as the Fourier coefficients violate the Picard condition. Additionally all solutions where the singular values have been filtered using Tikhonov regularization adhere to the Picard condition, which indicated that regularization was successful.

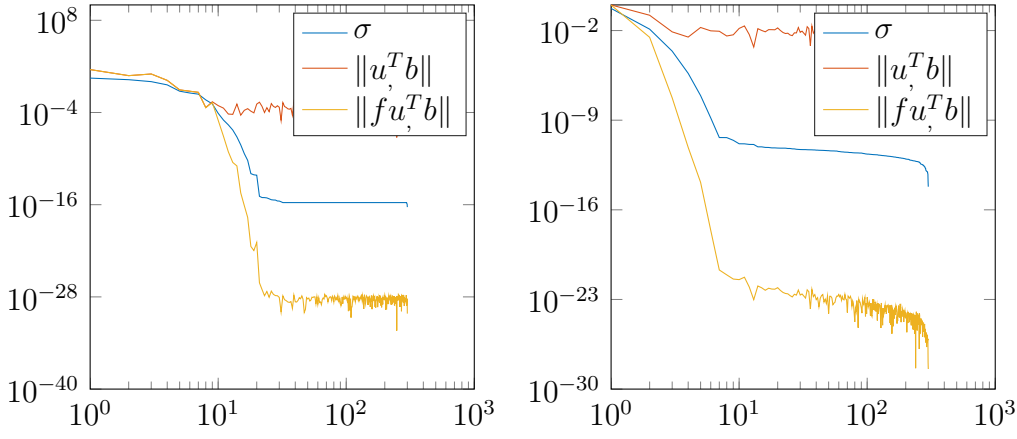


Figure 10: Plot of Fourier coefficients and singular values for the first  $\mathbf{A}_1, \mathbf{b}_{err1}$  and second  $\mathbf{A}_2, \mathbf{b}_{err2}$  value pair .

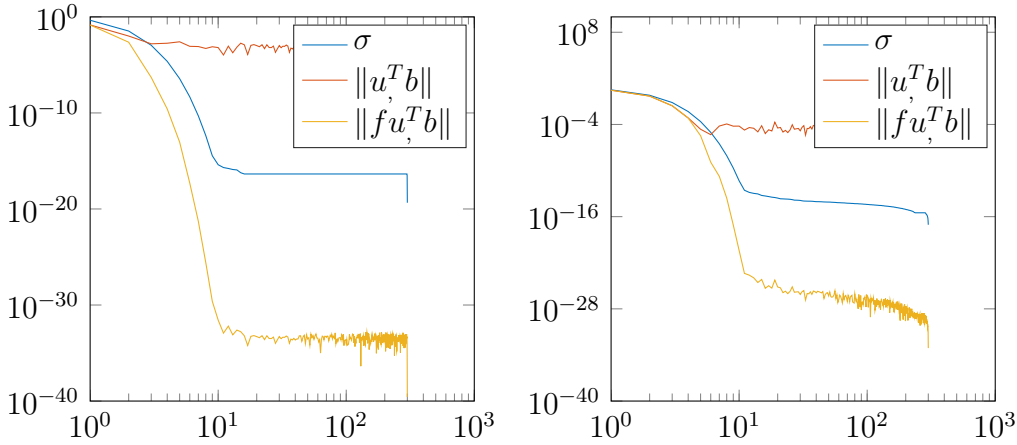


Figure 11: Plot of Fourier coefficients and singular values for the third  $\mathbf{A}_3, \mathbf{b}_{err3}$  and fourth  $\mathbf{A}_4, \mathbf{b}_{err4}$  value pair .

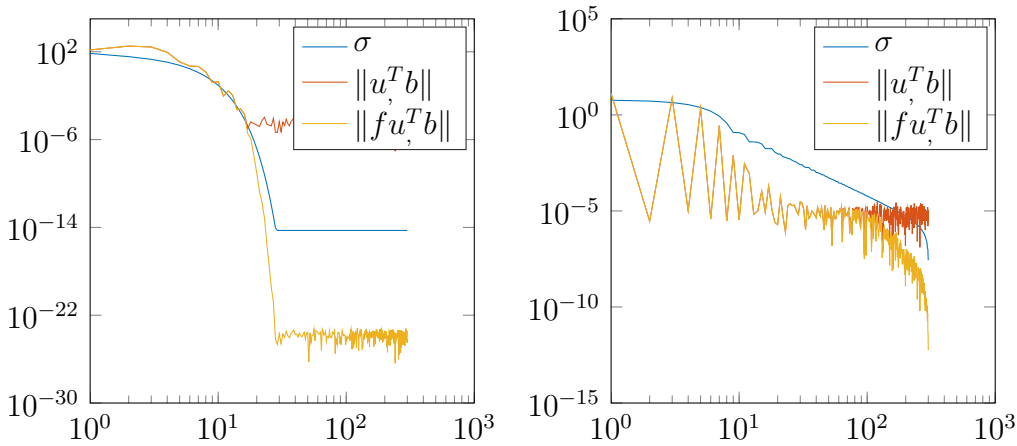


Figure 12: Plot of Fourier coefficients and singular values for the fifth  $\mathbf{A}_5, \mathbf{b}_{err5}$  and sixth  $\mathbf{A}_6, \mathbf{b}_{err6}$  value pair .



## 2.4 DSVD

A modification of the filter function given in equation 2 to

$$f_i = \frac{\sigma_i}{\sigma_i + \lambda} \quad (13)$$

gives the damped svd, which introduces less filtering. However the same effect can also be achieved by reducing the regularization parameter. Filtering following equation 13 has the drawback that often the L-curve is very noisy, which leads to curvature selection often incorrectly selecting a noise spike instead of the proper edge of the L-curve. Therefore dsvd has not been pursued further. A different approach is to truncate the svd after if the singular values are smaller the regularization parameter. Working with unfiltered matrices until they become stable will also lead to a noisy L-curve and has therefore not been pursued further.

## 2.5 Conjugate gradients

When solving normalized problems ( $\mathbf{A}^T \mathbf{A} \mathbf{x} = \mathbf{A}^T \mathbf{b}$ ) using the conjugate gradient (CG) algorithm solution components associated with large singular values appear first. While running the CG-algorithm the damping decreases from only using the largest singular values initially to using more and more in higher iterations. The listing below shows the way CG was implemented:

```
it = length(b);
r = A'*b;
p = r;
x = 0*p;
rsOld = r'*r;
for n = 1:it
    Asp = A'*(A*p);           % form A'*A without computing A'*A.
    vAlpha = rsOld/(p'*Asp);   % step length.
    x = x + vAlpha*p;         % approximate solution.
    r = r - vAlpha*Asp;       % residual
    rsNew = r'*r;
    vBeta = (rsNew)/(rsOld);   % improvement of previous step.
    p = r + vBeta*p;          % search direction.

    rsOld = rsNew;            % squared residual update.

    xVec(:,n) = x;           % store the solution
    resNormVec(n) = norm(A*x-b); % compute residual norm.
    solNormVec(n) = norm(x);  % compute the solution norm.
end
```

The code snipped above shows that in each iteration the residual norm and size of the solution are recoded. Observing the behavior of the algorithm reveals that

Figure 13 shows the results obtained from running the CG-algorithms on the  $\mathbf{A}_1, \mathbf{b}_{err1}$  pair. In comparison to figure 2 CG performs equally well as Thikonov regularization. The regularization parameter with CG is the number of iterations. As the norm values

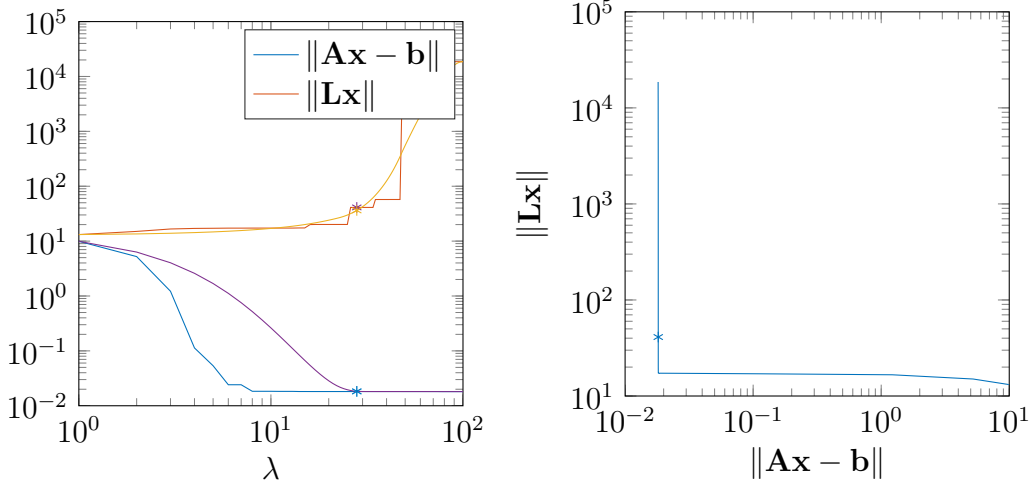


Figure 13: Result of conjugate gradient iterations on the  $\mathbf{A}_1, \mathbf{b}_{err1}$  pair. The yellow and purple lines show smoothed version of the orange and blue lines.

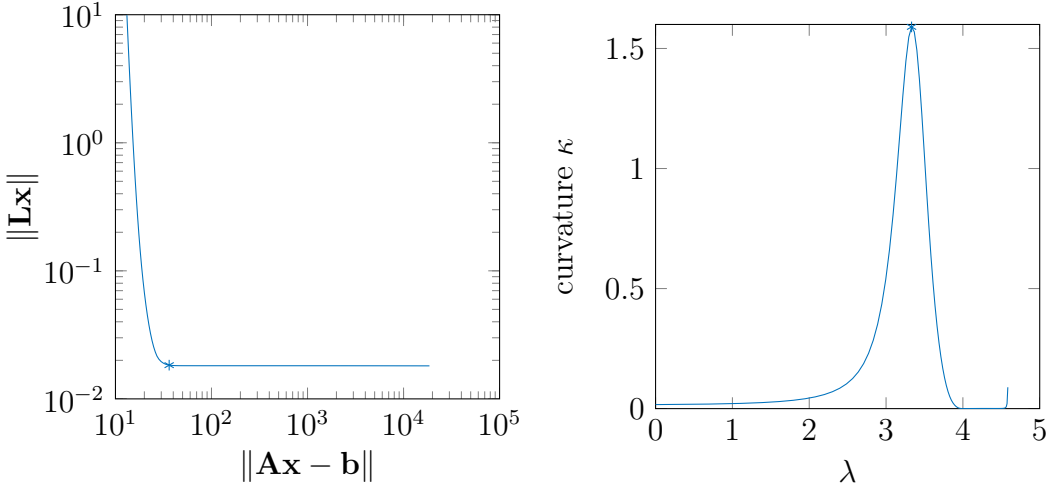


Figure 14: Smoothed L-curve and  $\kappa$  of this new L-curve.

for both norms are not continuous, using the L-curve criterion for selecting a suitable number of iterations is difficult, as it is very hard to find the edge of the L-curve. Using filtered approximations of the norm functions as shown in figure 13 on the left leads to the smoothed L-curve shown in figure 14. A meaningful curvature function can now be computed. The approximated edge of the L is indicated by a star as before. L curve plots from CG application to the remaining five data sets are shown in figure 15. L-curve shapes only appear for the sets two, three and four. For  $\mathbf{A}_5, \mathbf{b}_{err5}$  and  $\mathbf{A}_6, \mathbf{b}_{err6}$  the curve is an inverted A. Which indicates that the conjugate gradient method can only minimize residual only if  $\|\mathbf{Lx}\|$  becomes large, which implies undesired tracking of the noise contributions. For  $\mathbf{A}_2, \mathbf{b}_{err2}$ ,  $\mathbf{A}_3, \mathbf{b}_{err3}$  and  $\mathbf{A}_4, \mathbf{b}_{err4}$ , the CG-algorithms produces an L-shaped curve. For the second case the reduction of the solution norm is insufficient. In the third and fourth case results are comparable to Tikhonov regularization, however the approximations of the proper number of iterations could be more precise.

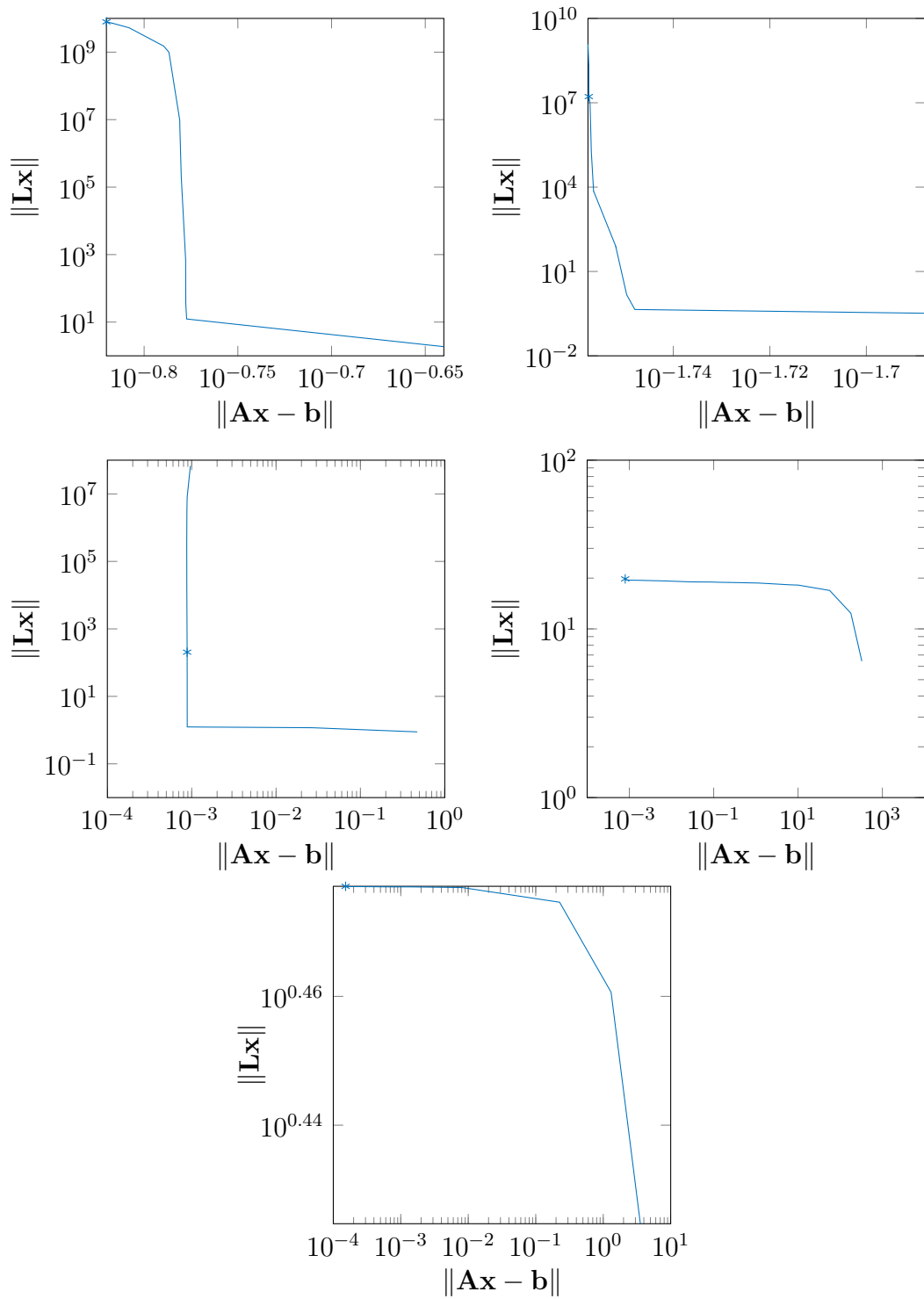


Figure 15: L-curve plots of the original CG-results on the five remaining pairs in increasing order, with edge approximation indicated by a star. The approximation comes from smoothed data, which is not shown.

### 3 Conclusion

In this report several different methods to regularize noisy problems have been discussed. To balance damping and oscillating of the solution the L-curve has been discussed. Including an automatic mechanism to pick a good regularization parameter. Tikhonov's method produced good results. The same method also worked with generalized cross validation. Tsvd, Dsvd and conjugate gradient methods produce noisy L-curves. Often these curves are equally good from a regularization point of view. But it is hard to choose a good regularization parameter automatically using curvature data computed from derivatives. Sometimes filtering of the noisy data can lead to acceptable approximations. The use of GCV in connection with these methods should be investigated further. It might prove to be more noise resistant. Due to time constraints this is outside of the scope of this report. Finally the Picard condition has been checked for filtered and unfiltered problems when using Thikonov regularization. Evaluation of the results provides reason to believe that all six problems have been correctly regularized.